T3.7-P12

The use of waveform cross correlation for detection, relative location and magnitude estimation of repeated mining blasts: the Jordan phosphate mine Eshidiya

Yochai Ben Horin[1], Dmitry Bobrov[2], Ivan Kitov[2], Mikhail Rozhkov[2], Matthew Yedlin[3]

[1]Soreq Nuclear Research Centre, [2]CTBTO Preparatory Commission for the Comprehensive Nuclear Test-Ban Organization, [3]University of British Columbia,

CTBTO PREPARATORY COMMISSION

Abstract

We analyze signals measured by seismic stations HRFI, PRNI, EIL, ASF, and MMAI from a long series of repeated blasts at the Eshidiya phosphate mine in Jordan. At first, we estimate the dependence of cross correlation coefficient on signal length and frequency band using all pairs of events detected at a given station. A small set of signals having the highest similarity with all other signals are used as waveform templates in detection based on waveform cross correlation. Three stations lie west of the phosphate quarry and have the same sampling rate. We cross-correlated signals from different stations and events and found high level of similarity, which is close to the level of similarity between signals at one station. For each event detected by three and more stations, we calculated location and magnitude relative to the selected master events. In order to characterize the overall similarity between signals we applied the Principle Component Analysis to waveforms at each station and found that the level of normalized eigenvalues falls to 0.2 and below for the first five to ten components. The PCA eigenvectors corresponding to the highest eigenvalues are successfully used as waveform templates since they can find all signals.

BLASTS AT ESHIDIYA MINE DETECTED AT STATION HRFI

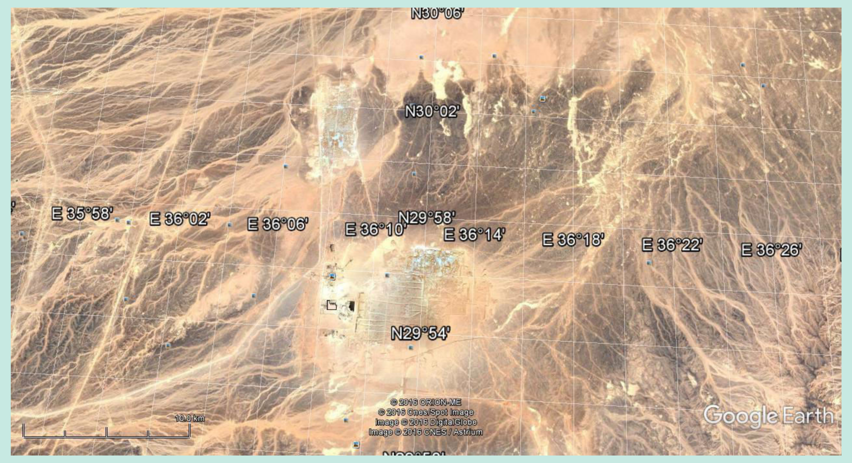

Figure 1. The phosphate mine **Eshidiya**, 70 km away from Ma'an District and 330 km from Amman, has been extracting fossils using chemical blasts since 1989. It has two sites with the largest possible distance between events of approximately 20 km, a challenge for detection using waveform cross correlation

Figure 2. A few thousand blasts were conducted within the quarry. For the study of waveform cross correlation, we have selected 1654 events (blue circles) with records at station HRFI. There are other stations measuring most of these events: PRNI, EIL, ASF, MMAI, which will be studied next.

Waveform cross correlation (WCC) is a powerful technique to detect and accurately locate repeated events. Quarries provide extensive series of waveforms characterized by a higher level of similarity since blasts are conducted within a few km from each other. The Jordan phosphate mine **Eshidiya** (see Figure 1) has a long history of blasting (since 1989), with thousands of events measured at near-regional distances by several seismic stations. These blasts have different yields, and thus, some of them produce stronger signals. The level of microseismic noise is also changing within a day and between seasons that changes detection conditions. Therefore, not all blasts can be detected even by the nearest stations. Another problem is association of detected signals with a given mine. Natural earthquakes around quarries can also be detected and wrongly associated with mining activity. Waveform cross correlation is able to separate blasts and natural events using the difference in waveform shape and/or differences in arrival times at several stations.

Here we study the level of similarity of waveforms from quarry blasts conducted at the Eshidiya mine since 2004 and detected at near-regional distances. We have selected the 3-component station HRFI of the Israel National Seismic Network operated by Geophysical Institute of Israel (GII Israel). HRFI is situated at a distance of approximately 130 km from the quarry, as Figure 2 illustrates, and has sampling rate of 40 Hz. We use 1654 signals for waveform cross correlation. Figure 2 depicts locations of these events as measured by the Israel National Seismic Network. These locations are characterized by high scattering around the mine, beyond the boundaries of the blasting area. Therefore, identification and accurate location of these events is a challenge for the WCC method.

We processed all 1654 seismograms using the standard detector STA/LTA with STA=0.5 s and LTA=20 s and detected all 1654 signals with SNR>4. Figure 3 presents spectrograms as obtained for the vertical channel of HRFI. To increase signal-to-noise ratio (SNR=STA/LTA) we used a set of filters covering the frequency bands between 1 Hz and 16 Hz: 1) 1-3 Hz, 2) 2-4 Hz, 3) 3-6 Hz, 4) 4-8 Hz, 5) 6-12 Hz, 6) 8-16 Hz. This set covers frequencies of observed signals: from P to Rg waves. Figures 4 and 5 depict the frequency distribution of SNR and detection filters, respectively. Just a few dozens of detections have SNR<10. At the same time, the peak SNR value varies between filters, with a larger part of P-wave detections observed at higher frequencies. To accommodate the observed differences in relative frequency content between the measured signals in calculation of cross correlation coefficients, we created waveform templates in all six frequency bands. Typical templates as obtained from the quarry blasts are show in Figure 6, which illustrates the difference in frequency content of the P- and S-wave arrivals as well as the difference in amplitudes of vertical and horizontal component. For waveform cross correlation, each blast from the 1654 can play the role of master and slave.

The studied blasts were conducted between January 2004 and January 2015. There is a gap in data between June 2007 and July 2010.

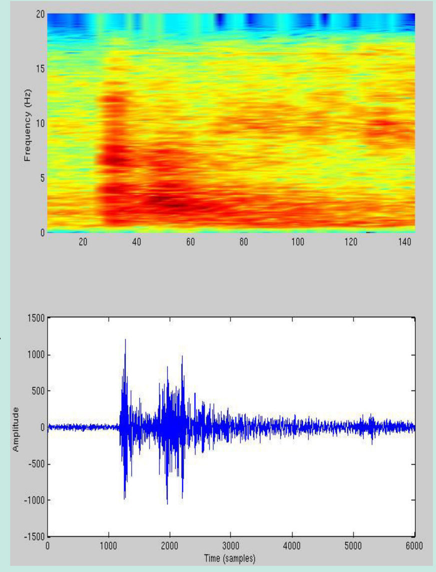

Figure 3. Spectrogram of a typical signal measured at vertical channel

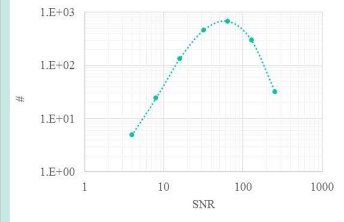

Figure 4. Frequency distribution of SNR of detected P-waves

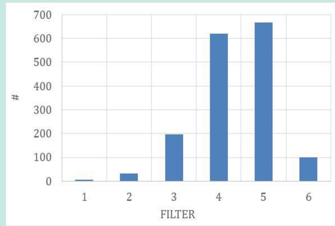

Figure 5. Frequency distribution of detections over filters

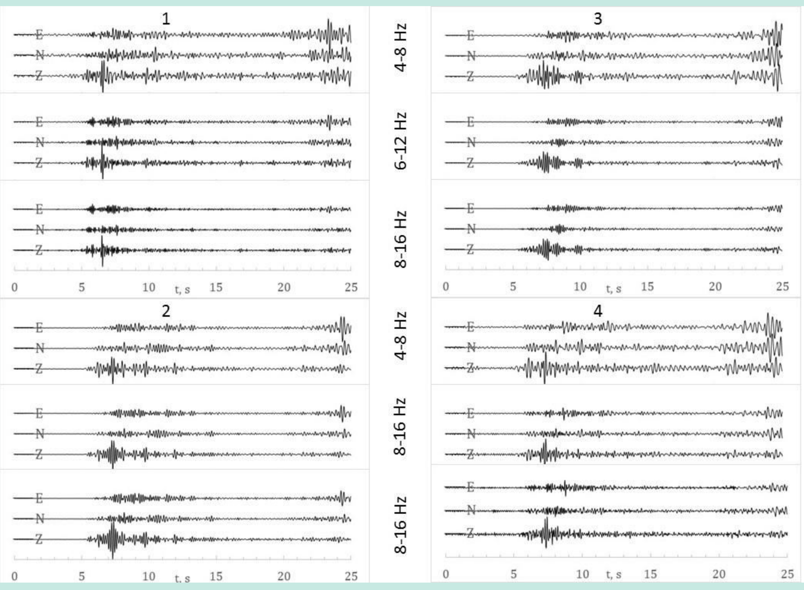

Figure 6. 3-C templates (E – east-west, N – north-south, and Z - vertical) as measured by HRFI from 4 blasts conducted within the quarry. Each waveform has been filtered in six frequency bands in order to obtain the highest signal-to-noise ratio. Three frequency bands are shown in the Figure. All templates include 5-second-long (200 samples) pre-signal segments.

DIMENSIONALITY REDUCTION : THE PRINCIPAL COMPONENT ANALYSIS

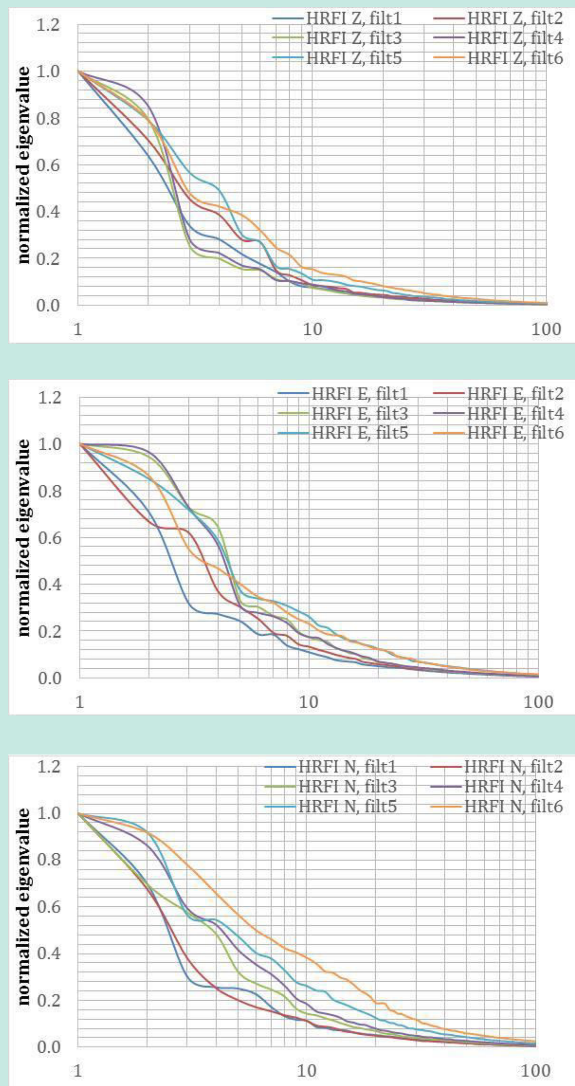

Figure 15. All eigenvalues obtained by SVD for 3 different components (E, N, Z) and 6 filters we normalized to their peak values. Only 100 components are shown in this Figure. For Z-component, normalized eigenvalues fall below 0.2 for PCA component 10.

The original signals are used to prepare waveform templates for cross correlation. Some of these templates demonstrate the highest possible detection rate with all slaves found for threshold SNR_{CC}>3.0 and even SNR_{CC}>3.75. Overall, the result of cross correlation implies high similarity between waveforms. Lower CC values for some master/slave pairs can be explained by the effect of similarity decreasing with distance and/or change in blast setting, but also by the influence of the ambient noise. The Principle Component Analysis (PCA) is a technique to obtain waveform templates retrieving similar features from all signals, which are also orthogonal to permanent features observed in the micro-seismic noise. Therefore, the use of templates obtained by the PCA may increase the average and minimal SNR.

We used all 1654 waveforms and the Singular Value Decomposition (SVD) method to calculate eigenvalues and eigenvectors. The latter are used as waveform templates. SVD was applied to three sets of signals measured at E-, N-, and Z-components and to each filter band separately. The length of waveform segment for the SVD was 75 s, and thus, all regular seismic phases were included.

Figure 15 illustrates the dramatic fall in eigenvalues for components beyond 10 to 15. The normalized eigenvalue drops below 0.2, and thus, the corresponding eigenvectors do not contribute much to the decomposed original waveforms. The behavior of the eigenvalues is in line with the result of detection in Figure 9 - the original waveforms are very similar.

The rate of fall in normalized eigenvalues is slightly different between components and filters, however. This observation makes it important to use all filters and components to prepare waveform templates. Figure 16 presents four 3-C templates as compiled from eigenvectors 1, 2, 5, and 10. The difference between vertical and horizontal components is expressed in relative amplitudes and frequency content. The Z-component of the P-wave is of relatively higher amplitude at higher frequencies, but this difference decreases with frequency. For the S-wave group, the E-component is the highest between 4 Hz and 8 Hz, but shear waves almost disappear at higher frequencies. The performance of the obtained PCA components should change with template length, filter, and the use of one or three components together. Therefore, we have to determine template settings optimal for detection.

At first, we calculated CC-traces and SNR_{CC} for eigenvectors from 1 to 100 using template length 15 s, i.e. the P-wave group before the S-wave arrival. Figure 17 shows the averaged SNR_{CC} estimates as obtained for the 3-C and Z templates. We have excluded SNR_{CC}<3.0, i.e. non-detections, from averaging process. The use of 3-C templates in cross correlation is likely more efficient as expressed by higher average SNR_{CC} observed for first two PCA components. The same effect is observed for the original templates. The difference between 3-C and Z-templates decreases with index. One also should not use for detection templates beyond the 10th because their performance is poor.

Figure 18 presents frequency distribution of detection filters (i.e. the filter with the highest SNR_{CC}) for the first ten PCA templates. For detection, the most effective is the filter between 8 Hz and 16 Hz (see Figure 16).

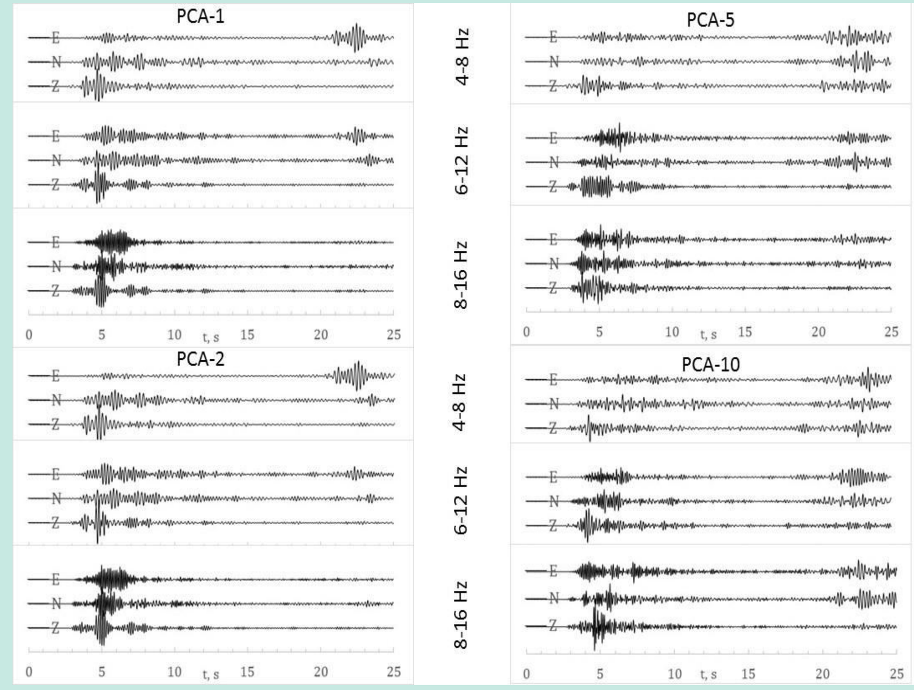

Figure 16. Four PCA templates (E – east-west, N – north-south, and Z - vertical) as compiled from eigenvectors 1, 2, 5, and 10, which were obtained separately for E-, N- and Z-components. Three frequency bands are shown in the Figure. All templates include 2.5-second-long (100 samples) pre-signal segments.

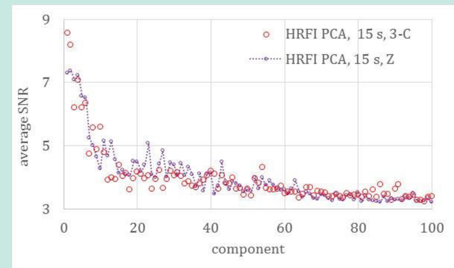

Figure 17. Comparison of the averaged SNR estimates as obtained for the 3-C and Z templates based on the PCA components 1 to 100. Non-detections are excluded. The average 3-C SNR estimates for the first two components are the largest. Templates 1 to 10 are the best in both cases.

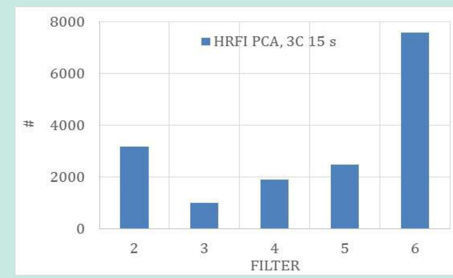

Figure 18. Frequency distribution of detection filters for the 3-C templates from 1 to 10. The filter between 8 Hz and 16 Hz is superior for detection with PCA.

WAVEFORM CROSS CORRELATION AT STATION HRFI

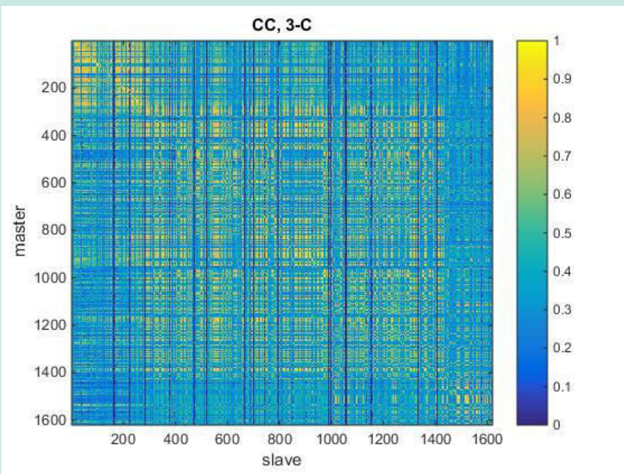

Figure 7. Maximum absolute CC-values for all master/slave pairs. There are clear clusters with CC close to 1, which are likely series of spatially close blasts. There are three distinct periods – 2004 to 2007 (upper left corner), 2010 to the end of 2013, and 2014 (lower right corner). There are events (as expressed by vertical blue lines) with low correlation with all other templates.

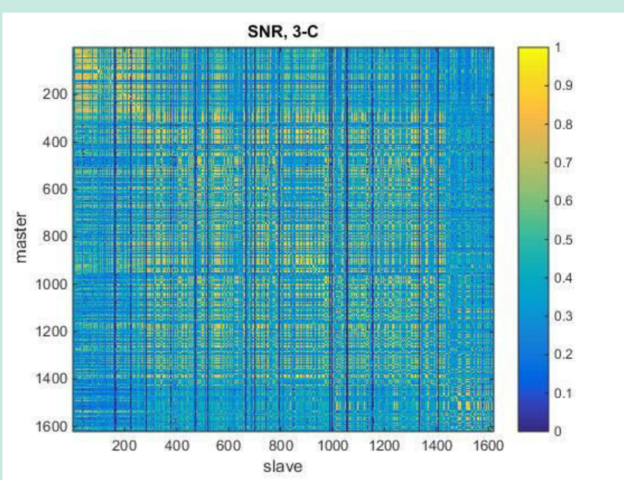

Figure 8. Maximum SNR_{CC} for all master/slave pairs. The highest SNR is observed for autocorrelation - diagonal elements. Window length is 15 s. Three highest frequency band are used.

At first, we calculated cross correlation coefficient for all pairs of events as masters and slaves using all three components (3-C) and Z-component only. This allows direct comparison of detection efficiency, with standard SNR_{CC}=STA/LTA>3.0 used as a detector threshold. We selected a time window of 15 s after the P-wave arrivals and filters from 2 to 6. The lower frequency filter between 1 Hz and 3 Hz is sensitive to the ambient noise, and thus, was excluded from our analysis.

Figures 7 and 8 illustrate the results obtained for 3-C cross correlation. There are three distinct blasting periods with different level of similarity between waveforms. Between 2004 to 2007 (upper left corner), majority of signals are characterized by high CC above 0.7, which is accompanied by high SNRs shown in Figure 8. The signals measured between 2010 and January 2014 are split in smaller clusters as expressed by high CC values. However, they do not correlate well with the signals measured between 2004 and 2007 and have lower correlation with the signals observed from January 2014 to January 2015 (lower right corner). It is important that there exist events, whose signals do not correlate with other waveform templates. These are likely the events with low SNR_{CC} in Figure 4. In some cases, cross correlation detection can be more efficient than that with original waveforms.

Figure 9 presents detection rates for all templates, i.e. the portion of slave events found by a given template. All templates have detection rate above 0.996 and there are 501 templates, which have found all slave signals with the detection threshold SNR_{CC}=3.0. The latter could serve for detection of signals from the studied quarry with the WCC method. One can select the best templates from 501 using the minimum SNR_{CC} values for a given template, which are shown in Figure 10. The largest value of SNR_{CC}min is above 3.75 and several templates can best serve for detection. Moreover, for any given slave the lowermost SNR_{CC} among all masters is around 8, i.e. much higher than the smallest SNR found by in original waveforms in Figure 4. For these two templates, the detection threshold can be increased to 3.5 with the perfect detection rate of 1. Higher detection thresholds are important for better discrimination between the studied quarry blasts and natural seismic sources as well as for effective elimination of false alarms associated with microseismic noise.

Figure 11 and 12 presents the average SNR_{CC} and CC for each template, with non detections (SNR_{CC}<3.0) excluded. Three different periods of blasting are clearly seen.

Figure 13 compares the detection performance of 10 best 3-C and Z-templates as expressed by SNR_{CC}min. The 3-C templates are characterized by higher values and provide larger SNR_{CC} threshold. Overall, the 3-C templates contain more information on signals and better suppress the ambient noise.

Figure 14 illustrates the difference in detection filters between 3-C and Z-templates. The most efficient filter is lower for 3-C templates since horizontal components (see Figure 6) are characterized by lower frequency content.

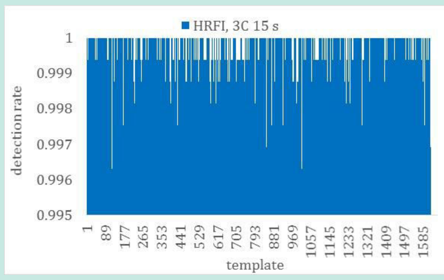

Figure 9. Detection rates for all templates. There are 501 templates which have found all slave signals with detection threshold SNR_{CC}=3.0

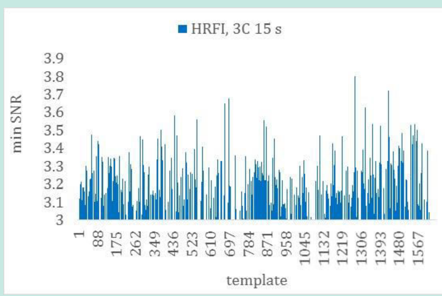

Figure 10. Minimum SNR_{CC} for all templates, which is 0 when at least one signal is not detected by a given template. The largest SNR_{CC}min is above 3.75, which can be used as the highest detection threshold with at least one template detecting all signals

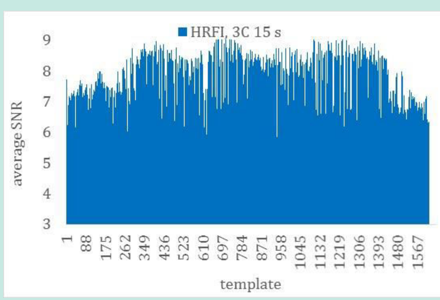

Figure 11. Average SNR_{CC} for all templates, with non-detections, i.e. SNR_{CC}<3.0, excluded. The largest mean SNR_{CC} is ~8.5, also with detection rate 1.0. The mean SNR_{CC} is significantly lower in the beginning of blasting (between 2004 and 2007) and during 2014.

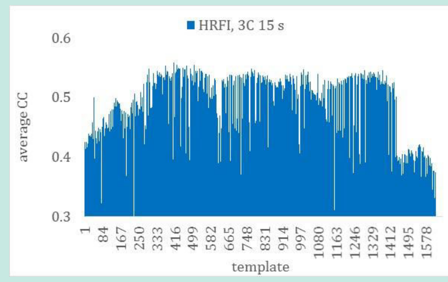

Figure 12. Average CC for all templates, with non-detections, i.e. SNR<3.0, excluded. Three periods and clusters are clear seen.

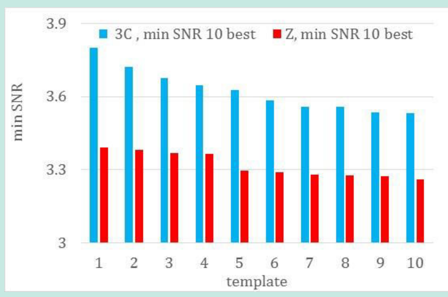

Figure 13. SNR_{CC}min for 10 best 3-C and Z- templates. The 3-C templates are superior, and thus, can provide larger SNR_{CC} threshold important for efficient signal separation from background noise.

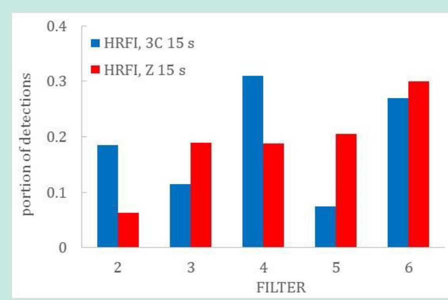

Figure 14. Distribution of detections over filters. For 3-C, the largest number corresponds to filter 4 Hz to 8 Hz, and for Z-component the peak is for the filter between 8 Hz and 16 Hz.

PERFORMANCE OF PCA TEMPLATES, SIMILARITY BETWEEN STATIONS, LOCATION

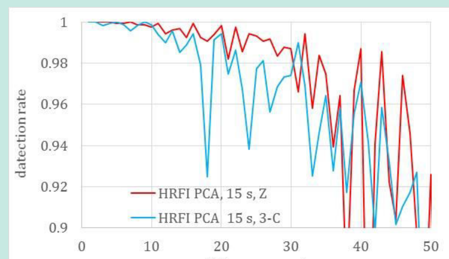

Figure 19. Comparison of detection rates for Z and 3-C templates from 1 to 50. The first three 3-C templates guarantee 100% detection rate.

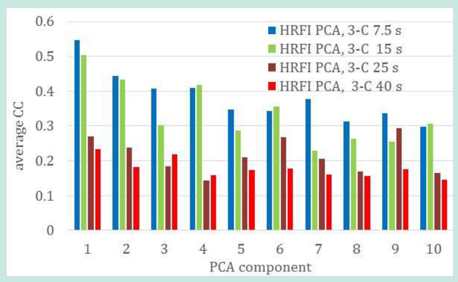

Figure 20. Comparison of average CC for different template lengths – from 7.5 s to 40 s. Shorter signals are characterized by higher CC

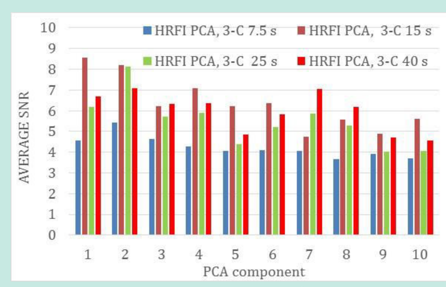

Figure 21. Comparison of average SNR for for different template lengths – from 7.5 s to 40 s. The length optimal for detection is near 15 s.

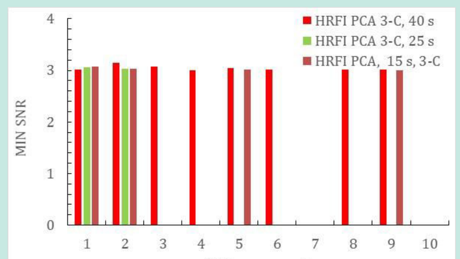

Figure 22. Comparison of minimal SNR_{CC} for different template lengths – from 7.5 s to 40 s. The largest SNR_{CC}min belongs to the longest window.

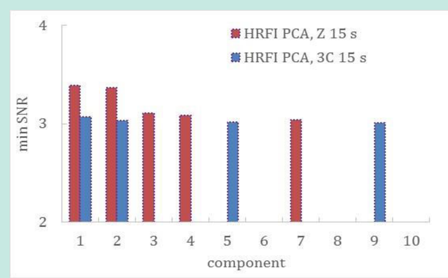

Figure 23. Comparison of min SNR for Z and 3-C templates.

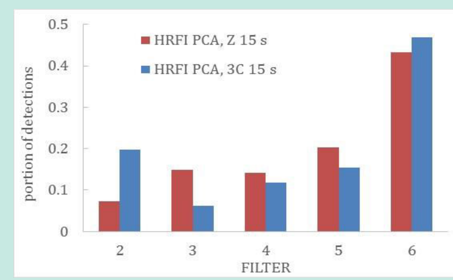

Figure 24. Distribution of detection filters for 10 first Z and 3-C templates as obtained from PCA eigenvectors. All in all, the Z-templates demonstrate an increasing portion of detections with frequency. For 3-C templates, there is a deeper minimum around the 3rd filter.

In Figure 19, we compare detection rates obtained for the first 50 Z and 3-C PCA templates. The first three Z templates guarantee 100% detection rate.

The first 10 average CC values for four different 3-C template lengths – from 7.5 s to 40 s are displayed in Figure 20. Overall, shorter templates produce higher CC. This is in line with increasing specificity of waveform templates as expressed by the product of frequency bandwidth and window length.

Figure 21 presents the estimates of average SNR_{CC} for first 10 3-C components. There exists an optimal window length expressing the trade-off between cross correlation with signal and noise suppression. Overall, for the HRFI principal components, this length is between 15 s and 25 s. For higher order components, the SNR_{CC} peak shifts to longer windows, however.

A more important detection characteristic is the minimum SNR_{CC} presented in Figure 22. It defines the detection threshold. For the shortest window of 7.5 s, there is no component with 100% detection rate. The largest SNR_{CC}min belongs to the longest window. When only the Z-component is used for cross correlation, the peak SNR_{CC}min value increases to 3.3, as Figure 23 shows.

The choice of optimal filters for efficient detection is an important task. Figure 24 depicts the portion of detections as obtained by filters from 2 to 6 for the 10 first Z and 3-C templates. The portion of detections obtained by the Z-templates increases with frequency. For 3-C templates, there is a deeper minimum around 3rd filter.

There are several near-regional stations, which also measured the same events: EIL, PRNI, ASF, MMAI. Cross comparison of these stations can reveal important similarities and differences in their waveforms. Figure 25 shows results of cross correlation between all pairs of signals measured at two stations - HRFI and EIL. The size of the SNR matrix is 1620x1235. This matrix demonstrates that EIL signals can be used as 3-C templates to detect signals at HRFI. This is an important observations revealing high level of similarity of regional signals at distances of tens of kilometers.

Figure 26 presents distribution of cross correlation coefficient between signals at stations EIL and first 100 SVD components calculated from all 1620 signals recorded at station HRFI. All 3-C templates are 15 s long. Similarity is high (around 0.6) for the first 10 to 15 components and then quickly falls below 0.3.

The geographical distribution of 5 stations allows effective relative location of quarry blasts using empirical travel times difference between arrivals detected by cross correlation, which also provide more accurate onset times. This is especially important for weak signals. Figure 27 depicts the distribution of RMS travel time residuals obtained for one of blasts conducted in January 2016 and measured by 4 stations: ASF, EIL, HRFI and MMAI. The epicentre of the located event is approximately 8 km far from the centre of the mine. This is an accurate location considering the number of stations and azimuthal gap. Currently, we test continuous detection, association and location of all events at the studied mine using waveform cross correlation.

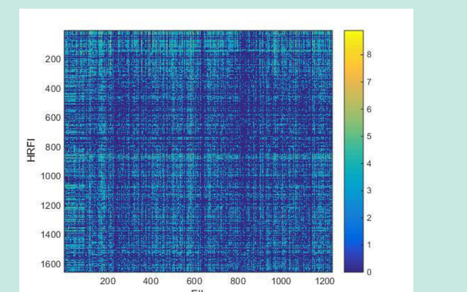

Figure 25. Signal-to-noise ration (SNR) for all pairs of signals recorded from all events measured at stations HRFI and EIL. All 3-C waveform templates were 15 s long.

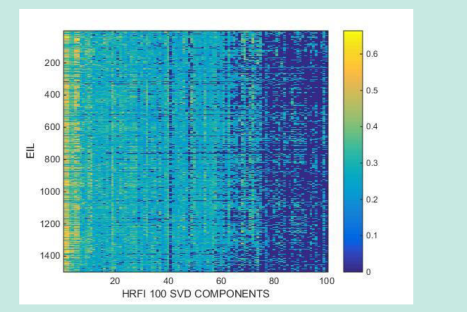

Figure 26. Cross correlation coefficient between EIL signals and first 100 SVD components for station HRFI.

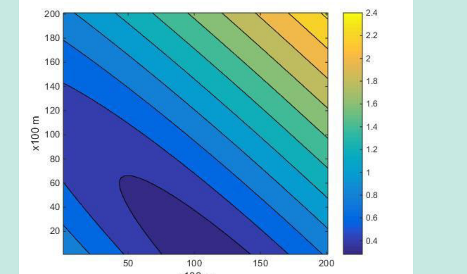

Figure 27. Distribution of travel time residuals obtained in relative location of one of the mining blasts using 4 stations – ASF, EIL, HRFI and MMAI. Scale in seconds. This event is approximately 8 km far from the assumed centre of mining activity.

Preparatory Commission for the Comprehensive Nuclear-Test Ban Treaty Organization, Provisional Technical Secretariat, Vienna International Centre, P.O. Box 1200, A-1400 Vienna, Austria. E-mail: ivan.kitov@ctbto.org

www.ctbto.org